

Clustering of aromatic rings in near-frictionless hydrogenated amorphous carbon films probed using multiwavelength Raman spectroscopy

R. Arenal and A. C. Liu

Citation: *Appl. Phys. Lett.* **91**, 211903 (2007); doi: 10.1063/1.2805189

View online: <http://dx.doi.org/10.1063/1.2805189>

View Table of Contents: <http://apl.aip.org/resource/1/APPLAB/v91/i21>

Published by the [American Institute of Physics](http://www.aip.org).

Related Articles

Comment on "Dynamics of glass-forming liquids. XIII. Microwave heating in slow motion" [*J. Chem. Phys.* **130**, 194509 (2009)]

J. Chem. Phys. **137**, 027101 (2012)

Solid-phase crystallization of ultra high growth rate amorphous silicon films

J. Appl. Phys. **111**, 103510 (2012)

Anomalous phase change characteristics in Fe-Te materials

Appl. Phys. Lett. **100**, 201906 (2012)

Molecular rotation in p-H₂ and o-D₂ in phase I under pressure

Low Temp. Phys. **37**, 1038 (2011)

The influence of overconstraint on the spatial distribution of mobility in an amorphous network

J. Chem. Phys. **135**, 194505 (2011)

Additional information on *Appl. Phys. Lett.*

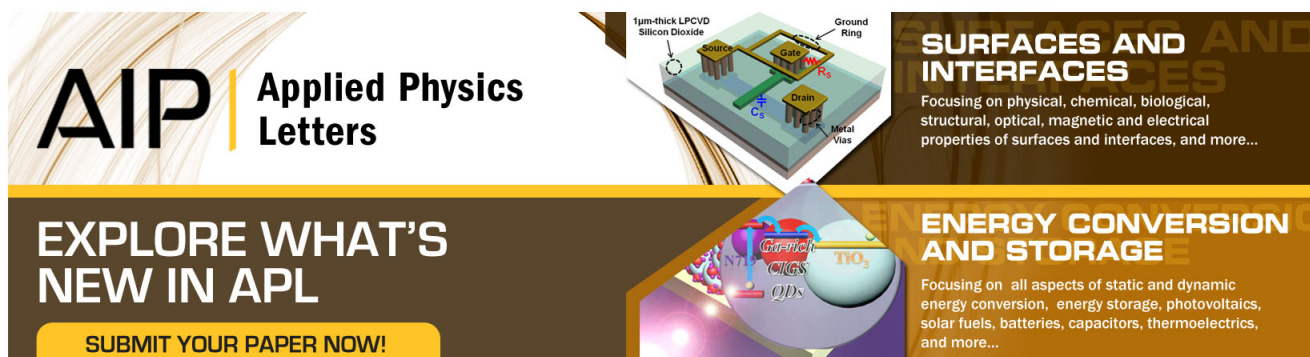
Journal Homepage: <http://apl.aip.org/>

Journal Information: http://apl.aip.org/about/about_the_journal

Top downloads: http://apl.aip.org/features/most_downloaded

Information for Authors: <http://apl.aip.org/authors>

ADVERTISEMENT



AIP Applied Physics Letters

EXPLORE WHAT'S NEW IN APL

SUBMIT YOUR PAPER NOW!

SURFACES AND INTERFACES
Focusing on physical, chemical, biological, structural, optical, magnetic and electrical properties of surfaces and interfaces, and more...

ENERGY CONVERSION AND STORAGE
Focusing on all aspects of static and dynamic energy conversion, energy storage, photovoltaics, solar fuels, batteries, capacitors, thermoelectrics, and more...

Labels in diagram: 1µm-thick LPCVD Silicon Dioxide, Source, Drain, Metal Vias, Ground Ring, QDs, CIGS, NO₂.

Clustering of aromatic rings in near-frictionless hydrogenated amorphous carbon films probed using multiwavelength Raman spectroscopy

R. Arenal^{a)}

Laboratoire d'Etude des Microstructures, ONERA-CNRS, 92322 Châtillon, France and Materials Science Division, Argonne National Laboratory, Illinois 60439, USA

A. C. Y. Liu

Materials Science Division, Argonne National Laboratory, Illinois 60439, USA

(Received 3 August 2007; accepted 12 October 2007; published online 21 November 2007)

Multiwavelength Raman spectroscopy has been used to study the structure of hydrogenated amorphous carbon films synthesized by plasma-enhanced chemical vapor deposition. The analysis of different parameters from the Raman spectra demonstrates that the diameter, structural, and topological orders of the sp^2 -bonded ring clusters increase with increasing fractions of hydrogen in the source gas. We report the existence of an unusual peak at 867 cm^{-1} that in such extended clusters of aromatic rings, could correspond to a graphitic mode activated by a relaxation of the phonon selection-rule resulting from defects. © 2007 American Institute of Physics.

[DOI: 10.1063/1.2805189]

Recent years have seen extensive investment in research on diamondlike carbon (DLC) materials due to their exemplary mechanical, tribological, chemical, and optical properties.¹ A DLC is a metastable, disordered carbon whose properties may be broadly tuned by adjusting the ratio of the carbon bonding hybridizations and the amount of hydrogen incorporated into the structures.² At Argonne, a near frictionless amorphous carbon (NFC) film with coefficients of friction ranging from 0.001 to 0.013 was grown by plasma-enhanced chemical vapor deposition.³ Originally, it was thought that the ratio of sp^2/sp^3 bonding and the percentage of hydrogen incorporated into the films (22–36 at. %) were key factors in producing the extremely low coefficients of friction in these unique films.^{3,4} However, fluctuation electron microscopy (FEM) measurements⁵ and simulations⁶ pointed to the potential importance of atomic clustering or medium-range order in determining film properties and behavior. Raman spectroscopy probes the atomic configurations in materials via the vibrational density of states (VDOS) and is a powerful technique to measure structural parameters such as bonding and structural order in amorphous carbons.^{6–9} In this work, we use Raman spectroscopy to examine the clustering in the NFC films.

In the first order region of the Raman spectrum of disordered C materials ($1100\text{--}1800\text{ cm}^{-1}$) are two peaks, denoted D and G, corresponding to breathing and stretching modes in sp^2 -bonded carbon clusters, respectively. The D peak at $\sim 1350\text{ cm}^{-1}$ implies whole aromatic rings with delocalization of the π bonds, while the G peak at $\sim 1580\text{ cm}^{-1}$ is produced by modes in either olefinic chains or aromatic rings. A third peak related to sp^3 sites may also be present in this region at 1332 cm^{-1} , corresponding to the T_{2g} mode. However, as the Raman scattering cross section is resonantly enhanced for sp^2 sites, in practice, this peak may be hard to observe and the first order region will be dominated by the structural configurations of the sp^2 bonded carbon. A series of careful experiments on a wide range of both DLCs and hydrogenated DLCs has demonstrated that monitoring differ-

ent parameters from the peaks in the first order region of Raman spectra can give insights into the proportion and clustering of the sp^2 phase.^{8–10} A thorough characterisation of clustering requires a multiwavelength Raman study¹⁰ as we present here.

The NFC films studied in this work are identical to those previously characterized by transmission electron microscopy techniques such as FEM and electron energy loss spectroscopy⁵ (EELS) that were grown with different fractions of H in the source gas composition. The source gas atmospheres employed and corresponding coefficients of friction are summarized as follows: 75% H_2 :25% CH_4 (0.001), 50% H_2 :50% CH_4 (0.004), 100% CH_4 (0.0140), and 100% C_2H_2 (0.27).^{3,4} The previous FEM studies demonstrated that in the bulk of these films, the atomic clustering increased as the overall proportion of H in the source gas atmosphere was increased. Here, we study clustering of the sp^2 bonded carbon using Raman spectroscopy. Unpolarized Raman spectra were collected using 244 nm and 514.5 nm light. A Jobin-Yvon Labram HR800 UV spectrometer with a $40\times$ objective lens and a Jobin-Yvon Labram HR800 visible spectrometer with a $100\times$ objective lens were employed, yielding spot sizes and spectral resolutions of $\sim 2\text{ }\mu\text{m}$ and $\sim 1\text{ }\mu\text{m}$ and 6 and 1 cm^{-1} for the UV and visible Raman studies, respectively. In both cases, the spectra were recorded in a backscattering geometry at room temperature with precautions taken to avoid sample damage. The spectra were fitted using Gaussian line shapes and the parameters of interest were extracted.

Figures 1(a) and 1(b) show a set of Raman spectra collected from the NFC films at 514.5 and 244 nm, respectively. Typical for such films, we see that the first order region consists of a broadband ($1100\text{--}1800\text{ cm}^{-1}$) due to the overlap of the D and G peaks, indicating the presence of sp^2 sites in sixfold aromatic rings and in both chains and rings, respectively. The second order spectral regions are also displayed in Fig. 1(a) and correspond to an overlap of 2D, D+G and 2G peaks. All the peaks are superimposed on a broad and sloping photoluminescence (PL) background that increases with increasing H content in the source gas. Indeed,

^{a)}Electronic mail: raul.arenal@onera.fr

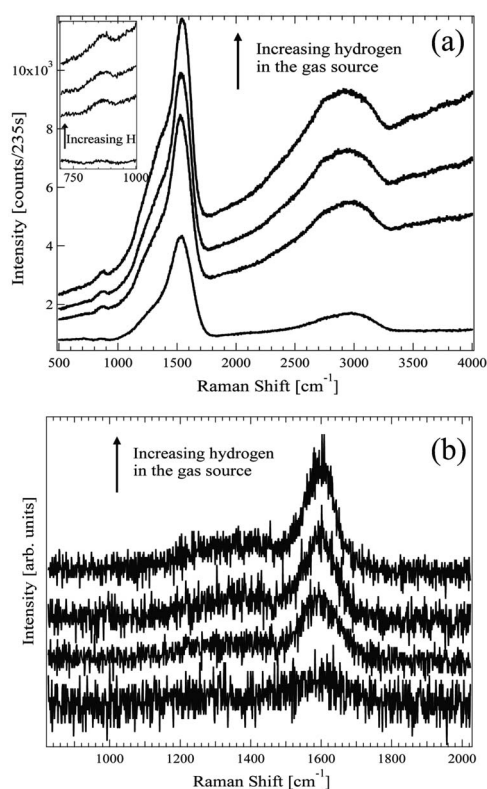


FIG. 1. (a) Visible (514.5 nm) and (b) UV (244 nm) Raman spectra of NFC films. A magnified view of the visible Raman spectra in the range of 700–1000 cm^{-1} is shown as an inset to (a). D and G peaks are clearly evident on top of an increasing PL background. Parameters of the D and G peaks are extracted from the spectra and shown in subsequent figures.

the total scattered intensity increases with increasing H in the source gas, indicative of a decrease in the optical absorption. This point is particularly evident in the UV Raman spectra, Fig. 1(b), where clearly the spectral intensity increases with increasing hydrogen content. We plot the gradient of the PL background, m , normalized to the intensity of the G peak, $I(G)$, in Fig. 3(c) to examine the trend in H content of these films.¹⁰ We see that as the H content in the source gas is increased, the amount of H incorporated into the films also increases. This is in line with previous determinations,⁴ that are plotted on the right ordinate.

We remark the presence of a more unusual peak at 867 cm^{-1} in the visible Raman spectra, which occurs in the three spectra from the films with higher H content (shown magnified in the inset to Fig. 1(a)). This peak can be also observed in spectra from similar films recorded by Casiraghi *et al.*, but its presence was not mentioned in this work.¹⁰ In single crystals, only phonon modes with wave vector $k=0$ contribute to Raman scattering. The presence of defects can lead to a relaxation of this $k=0$ selection rule, and provide a mechanism for phonon modes from outside the center of the Brillouin to contribute to the Raman scattering. Such a mechanism may explain the presence of this peak in the NFC Raman spectra. Other supportive examples may be found. A peak at this position was observed in highly oriented pyrolytic graphite (HOPG) samples,¹² in boron doped HOPG (Ref. 13) and in carbon onions.¹⁴ In the first example, this peak was thought to correspond to the B_{2g} mode which became active due to a change in the crystal point symmetry at the edges of graphite layers. In the case of the boron doped HOPG materials, the authors assign this mode to an A_{2u} in-

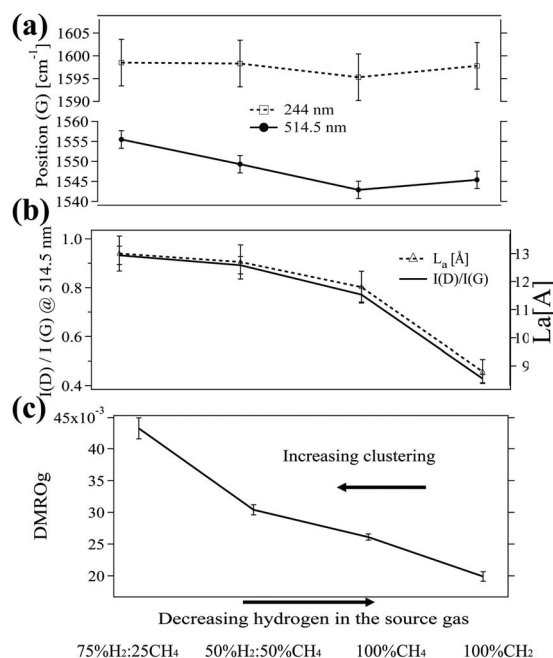


FIG. 2. (a) Position(G) as a function of the hydrogen content in the source gas from UV and visible Raman spectra. (b) $I(D)/I(G)$ as a function of the hydrogen content in the source gas from visible Raman spectra. (c) DMROg of graphitic clusters from previous FEM study. (Ref. 5).

frared mode¹⁵ that became Raman active due to the distortions of the hexagonal graphite lattice by the boron atoms which break the local symmetry of the graphite. In the last example of the carbon onions, this peak was attributed to a TO mode that became active due to the effect of curvature of the graphene planes.¹⁴ All these explanations imply the presence of quite large clusters of π -bonded rings in which extended crystal modes may be excited that are fundamentally different to the $k \neq 0$ modes that arise in disordered carbons due to the breakdown in translational symmetry. In the subsequent sections we will study clustering more closely.

Generally, for an amorphous carbon in stage 3 of the “amorphization trajectory” described by Ferrari and Robertson,⁹ at a given excitation wavelength, the position of the G peak, Position(G), will decrease as the clustering of the sp^2 -bonded carbon increases from dimers, to chains to rings.^{9,10} In Fig. 2(a), we plot the variation of the Position(G) against the H content in the source gas for both excitation wavelengths (244 and 514.5 nm). The UV data are the same within the spectral resolution (6 cm^{-1}). There is a trend in the visible data above the level of the uncertainty in the wavenumber, that would suggest that the degree of clustering increases with decreasing H in the source gas. However, there is a large degree of nonuniqueness in the trajectories that carbon materials take toward ordering or amorphization, especially at the boundary between stages 2 and 3 where, these films, with their low sp^3 contents may well reside.^{9,10} In this sense, Position(G) at a single wavelength is not the most reliable measure of clustering and we must measure other parameters.

As the D peak is related only to aromatic rings and the G peak corresponds to either rings or chains, the growth of the intensity of the D peak in relation to the G peak, demonstrates increased order or size in sp^2 bonded clusters.^{9–11} We plot the ratio of the D peak intensity to the G peak intensity, $I(D)/I(G)$, against increasing H content, in Fig. 2(b) show-

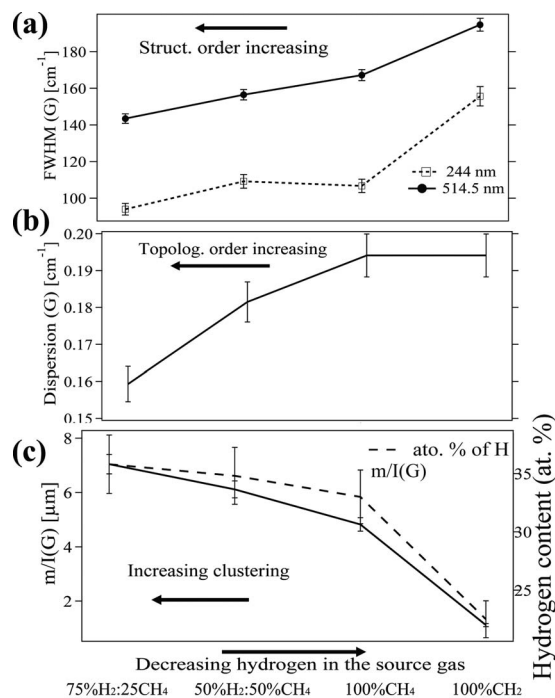


FIG. 3. (a) FWHM(G) from UV and visible Raman spectra and (b) dispersion(G) as a function of the hydrogen content in the source gas. A greater amount of hydrogen in the amorphous network promotes increased structural and topological orderings in the sp^2 -bonded clusters. (c) $m/I(G)$ as a function of the hydrogen content in the source gas. Increased hydrogen in the source gas gives rise to a greater amount of hydrogen incorporated in the final film.

ing that the clustering of the aromatic rings increases with H content. In addition, we may use an empirical expression to deduce the cluster diameter (or the in-plane correlation length L_a) from this parameter.⁹ These values are shown in the right ordinate of Fig. 2(b) and demonstrate that the size of the clusters varies from 13 to 9 Å. For comparison, we also plot the degree of medium-range order (DMRO) in graphitic clusters obtained from FEM measurements on cross-sectional specimens⁵ in Fig. 2(c). DMRO is a parameter related to the size, structural order within, or number of clusters. We see that DMRO also increases with increasing H content, in full agreement with the Raman results. The fact that the curves show different behaviors is due to the different ways they access the structural information.⁶ Raman spectroscopy probe structure via the VDOS, while FEM accesses this information from the phase shifts of electrons elastically scattered by atoms in different positions. Furthermore, simulations of the FEM data suggest that the sp^2 -bonded carbon exists in quite extended clusters of aromatic rings, providing a verification for the cluster diameters derived from $I(D)/I(G)$.⁶

Raman spectroscopy at a given wavelength will excite modes in clusters of a certain size. Strain or defects in these clusters will give rise to a larger G peak width (FWHM(G)), meaning that this parameter is intimately related to the structural order or bond length variations and bond angle distortions. We plot FWHM(G) against H content in Fig. 3(a), showing that the structural order also increases with increasing H content.

Dispersion of the G peak (Dispersion (G)) is evidence for a range of chain lengths that are resonantly excited as the wavelength is varied. If all the sp^2 -bonded carbon is present

in rings with fully delocalized π bonds, then this parameter is zero.¹⁰ Thus Dispersion(G) is a measure of topological order or the size and shape of sp^2 -bonded clusters. Figure 3(b) displays Dispersion(G) with H content. We see that the topological order also increases with increasing H content. We deduce that the degree of π delocalization is higher for the films containing a larger proportion of H. The optical gap is controlled by the degree of π delocalization.⁹ In the NFC films, the optical gap decreases with increasing H content. This supports the observation that the Raman scattering intensity increases with the H content as we saw in Fig. 1(a).

In summary, we have performed a multiwavelength Raman spectroscopy study on NFC films containing varying hydrogen contents. We demonstrated that the size, topological, and structural ordering of the sp^2 -bonded clusters increased with increasing amounts of hydrogen. These results independently confirm our recent FEM studies^{5,6} that measure higher graphitic DMRO in the films containing higher proportions of H . We discovered a peak at 867 cm⁻¹ in the visible Raman spectra from films that possess a H content higher than 30% and display more significant clustering. This peak can be attributed to the relaxation of the Raman selection rules in graphite due to defects in the sp^2 aromatic rings and implies quite extensive clustering of aromatic rings. Thus, we identify a significant structural change in the NFC films that occurs after the H content surpasses a threshold value. Overall, we observe that hydrogen in the amorphous network stabilizes larger sp^2 -bonded clusters and contributes to their structural and topological perfection. The presence of such extended clusters may be a factor in the exceptionally low dynamic coefficients of friction observed in such films.

This work was supported by the U.S. Department of Energy, Office of Science, under Contract No. DE-AC02-06CH11357. We thank A. Erdemir, O. Eryilmaz, J.A. Johnson, and J.B. Woodford for the NFC samples. We also express our gratitude to G. Montagnac of the Ecole Normale Supérieure de Lyon for assisting with the Raman spectroscopy.

- ¹J. Robertson, Mater. Sci. Eng., R. **37**, 129 (2002).
- ²C. Casiraghi, J. Robertson, and A. C. Ferrari, Mater. Today **10**, 44 (2007).
- ³A. Erdemir, O. L. Eryilmaz, and G. Fenske, J. Vac. Sci. Technol. A **18**, 1987 (2000).
- ⁴J. A. Johnson, O. L. Eryilmaz, X. Chen, J. Andersson, A. Erdemir, and J. B. Woodford, J. Appl. Phys. **95**, 7765 (2004).
- ⁵A. C. Y. Liu, R. Arenal, D. J. Miller, X. Cheng, J. A. Johnson, O. L. Eryilmaz, A. Erdemir, and J. B. Woodford, Phys. Rev. B **75**, 205402 (2007).
- ⁶A. C. Y. Liu, R. Arenal, and X. Chen, Phys. Rev. B **76**, 121401(R) (2007).
- ⁷A. J. Papworth, C. J. Kiely, A. P. Burden, S. R. P. Silva, and G. A. J. Amaratunga, Phys. Rev. B **62**, 12628 (2000).
- ⁸A. C. Ferrari and J. Robertson, Phys. Rev. B **64**, 075414 (2001).
- ⁹A. C. Ferrari and J. Robertson, Phys. Rev. B **61**, 14095 (2000).
- ¹⁰C. Casiraghi, A. C. Ferrari, and J. Robertson, Phys. Rev. B **72**, 085401 (2005).
- ¹¹R. Arenal, G. Montagnac, P. Bruno, and D. M. Gruen, Multiwavelength Raman Spectroscopy of Diamond Nanowires Present in n -type Ultrananocrystalline Films Phys. Rev. B (in press).
- ¹²Y. Kawashima and G. Katagiri, Phys. Rev. B **59**, 62 (1999).
- ¹³Y. Wang, D. C. Alsmeyer, and R. L. McCreery, Chem. Mater. **2**, 557 (1990).
- ¹⁴D. Roy, M. Chhowalla, H. Wang, N. Sano, I. Alexandrou, T. W. Clyne, and G. A. J. Amaratunga, Chem. Phys. Lett. **373**, 52 (2003).
- ¹⁵R. J. Nemanich, G. Lucovsky, and S. A. Solin, Solid State Commun. **23**, 117 (1977).